Experimental studies of East-West effect of the charge ratio of atmospheric muons with energies relevant to the atmospheric neutrino anomaly

I.M.Brancus[1], J.Wentz[1,2], B.Mitrica[1], H.Rebel[2,3], M.Petcu[1], A.Bercuci[1,2], C.Aiftimiei[1], M.Duma[1], and G.Toma[1]

[1] IFIN-HH, RO-76900 Bucharest, POB MG-6, Romania
[2] Forschungszentrum Karlsruhe, POB 3640, 76021 Karlsruhe, Germany
[3] University of Heidelberg, 69120 Heidelberg, Germany

The charge ratio of atmospheric muons is a quantity sensitive to hadronic interactions of cosmic rays and to the influence of the geomagnetic field. Experimental information is of current interest for tuning models used for calculations of the atmospheric neutrino fluxes. We report about experimental studies based on the observation of the life time of the muons stopped in the absorber layers (aluminium support) of a detector WILLI, consisting of 16 plastic scintillator modules (90 x 90 cm^2), surrounded by veto counters. The detector is mounted in a rotatable frame and installed in IFIN-HH Bucharest (vertical geomagnetic cut-off rigidity of 5.6 GV). Measurements of the asymmetry of the muon charge ratio in the East-West directions, observed with a mean zenith angle of 35^0, results in values of the asymmetry of the charge ratio decreasing from 0.25 to 0.20 in the muon momentum range of 0.35-0.50 GeV/c, relevant to the atmospheric neutrino anomaly.

1. Introduction

The atmospheric flux of muons originates from the decay of charged pions and kaons produced by cosmic rays in the atmosphere and is nearly isotropic.

$$\pi^{\pm} \rightarrow \mu^{\pm} + \nu_\mu\ (\overline{\nu}_\mu)\quad 100.0\ \%\quad \text{lifetime}\quad 2.6 \times 10^{-2}\ \mu s$$
$$K^{\pm} \rightarrow \mu^{\pm} + \nu_\mu\ (\overline{\nu}_\mu)\quad 63.5\ \%\quad \text{lifetime}\quad 1.2 \times 10^{-2}\ \mu s$$

Muons have a relatively large lifetime $\tau_0 = 2.2\ \mu s$, decaying in:

$$\mu^+ \rightarrow e^+ + \nu_e + \overline{\nu}_\mu$$
$$\mu^- \rightarrow e^- + \overline{\nu}_e + \nu_\mu$$

At lower energy the muon flux is influenced by of the local magnetic field as well by the magnetic rigidity cut-off of the primary cosmic rays penetrating the Earth's atmosphere from the cosmos /1/. Considering the decay chains, it is obvious that the ratio of positive to negative atmospheric muons, called the muon charge ratio $R_\mu = \mu^+/\mu^-$ carries information on the hadronic interactions (used for the calculations of the fluxes) and on neutrino production. Super-Kamiokande /2/ and other experiments find that the ratio of muon neutrinos to electron neutrinos is much smaller than the theoretical predictions; the effect is depending on the angle of incidence of the neutrinos. A possibility to verify the interaction models, invoked for neutrino flux calculations, is to compare the theoretical results for the muon flux, with the experimental data /3/. The compilation of muon charge ratio values over several decades shows that at higher energies all experiments are consistent with a value $R_\mu \approx 1.3$. At energies lower than 1.0 GeV, the experimental uncertainities appear to be larger and the data disagree with each other. The influence of the Earth's magnetic field leads to an asymmetry of low energy positive and negative muons due to different tracks of the particles. This finding led us to perform directional measurements of muon charge ratio in this energy range.

2. The method and WILLI detector

The WILLI (Weakly Ionising Lepton Lead Interactions) detector is installed in IFIN-HH Bucharest, Romania, *located at $44^0 26'$ N latitude, $26^0 04'$ E longitude, about 80 m above sea level, the vertical geomagnetic cut-off is 5.6 GV.*

Our method /4/ to determine the muon charge ratio is based on the different behaviour of positive and negative muons stopped in matter: while positive muons decay with their natural life, the negative muons are captured in atomic orbits and form muonic atoms, leading to a shorter lifetime of the negative muons in matter.

The WILLI detector, built IFIN-HH Bucharest**,** measures the effective life-time of the stopped muons for both charge states by observing the appearance of decay electrons and positrons after the muon stopped.

Fig. 1 presents the initial configuration of WILLI /5/ using 16 modules for vertical measurements of muon charge ratio, and 4 scintillator modules in vertical position as anticounters for background rejection.

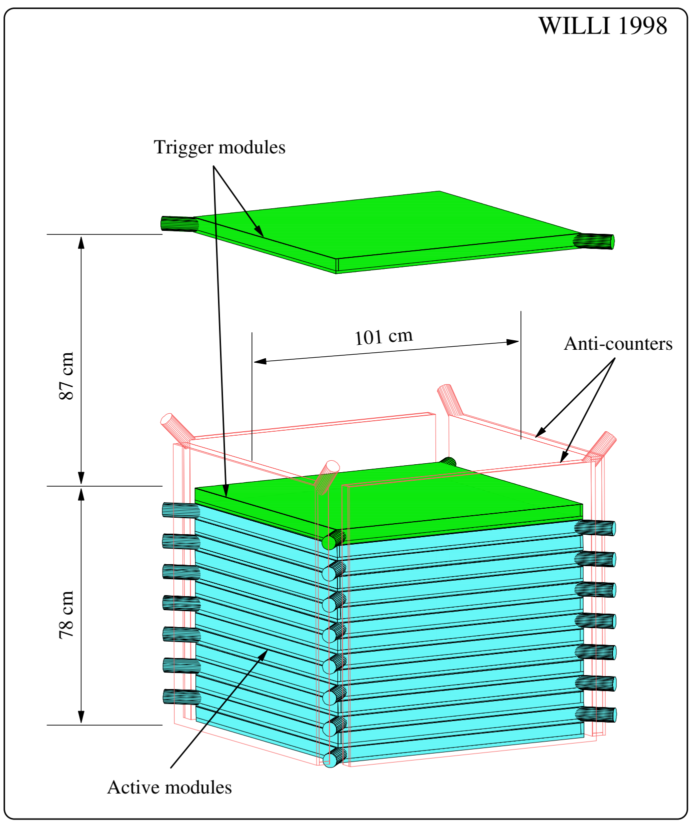

Fig.1 The vertical WILLI detector

The WILLI detector has been modified and transformed in a compact rigid detector with rotating facilities in zenithal and azimuthal direction /6/.

Fig. 2 presents the new rotatable WILLI detector installed in a frame which permits rotation and inclination for performing charge ratio measurements for muons with different angles-of-incidence.

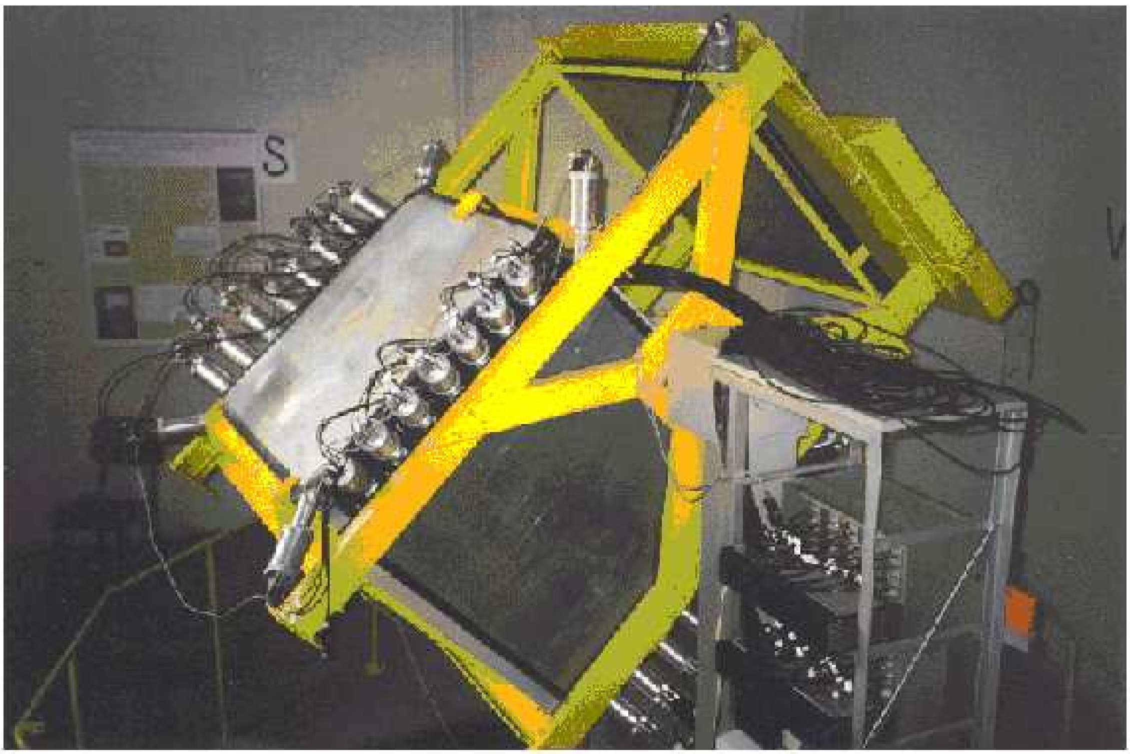

Fig.2 The rotatable WILLI detector

The detector is equipped with 40 photomultipliers providing energy deposit and time information. The trigger is made out of four separate signals corresponding to two of the detector layers, which define also the acceptance of the device.The light from each scintillator layer is collected by 4 wave length shifters (one for each side of the plate) towards the photomultipliers placed in opposite corners. From each photomultiplier three signals are taken out: one time signal from the first dynode and two amplitude signals from the anode and the third dynode. The signal from the third dynode allows the increase of the energy dynamic measurement with a factor of 10. The 80 amplitudes signals are sent in ADC modules. The time signals of 40 ns widths are sent in a 32 inputs MTDC module (Multiple Time digital Converter) which memorise the time evolution of each event in a limited time interval of 51.2 μs. A FIFO memory 2048 x 32 bytes with 25 ns resolution is used by means of a 40 MHz oscillator.

3. Monte Carlo simulations and measurements for vertical muons

The total decay curve of all muons measured in the detector is a superposition of several decay laws, /4,5/, containing 3 detector dependent constants c_j, accounting for the stopping power in the materials and the detection efficiencies, given by the detector geometry, laboratory walls, thresholds and angular acceptance, which have been determined by extensive detector simulations using the code GEANT /7/:

$$\frac{dN}{dt} = \frac{N_0}{R+1}\left[Rc_0 \frac{1}{\tau_0} \exp\left(\frac{-t}{\tau_0}\right) + \sum_j c_j \frac{1}{\tau_j} \exp\left(\frac{1}{\tau_j}\right)\right]$$

where, R represents the muon charge ratio, $N_0 = N^+ + N^-$, where N^+ , N^- are the numbers of positive and negative muons, respectively, τ_j indicates the lifetime for μ^- with the index j describing the absorber and the index 0 standing for positive muons and c_0, c_j are the detection efficiency constants for μ^+ and μ^- in the material.

The simulations have shown that aluminium is a material which discriminates well between the positive and negative muons, as it significantly reduces the life time for negative muons and it remains a sufficiently large decay probability (39,5 % for Al, as compared with 2.75% for Pb) .

Fig. 3 presents the measured data with vertical WILLI compared /5/ to other recent experiments /8/.

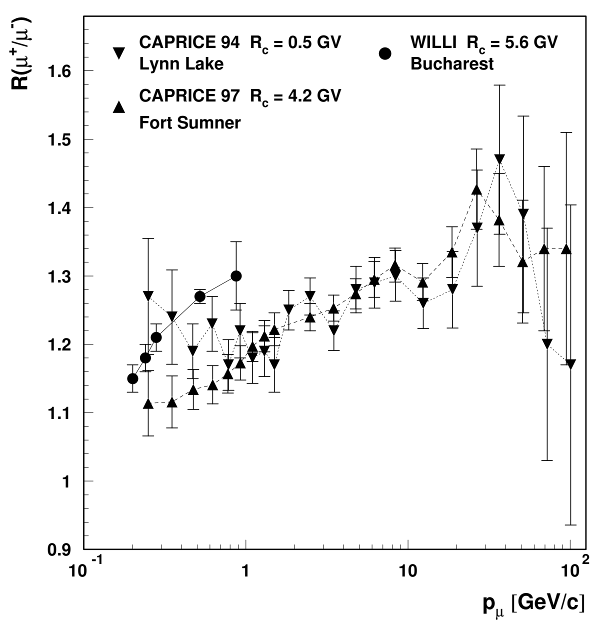

Fig.3 The WILLI results for the muon charge ratio at sea level together with recent results from CAPRICE experiment for two locations with different cut-off rigidities

The WILLI results show a smooth decrease of the charge ratio towards lower energy, which could be expected in terms of the geomagnetic cut-off; the muon charge ratio values are larger than the CAPRICE results for Fort Sumna, New Mexico at nearly the same geomagnetic cutoff and they are partially larger than CAPRICE results for Lynn

Lake, Canada where actually no cut-off effect and decrease should be expected. The decrease in the CAPRICE values with an indicated modulation is hardly understandable.

4. The rotatable WILLI detector

Fig. 4 shows the signature of an event, representing a stopped and decaying muon, which is a particle triggering the telescope, but not penetrating till the bottom of the scintillator stack, together with the appearance of a delayed particle, disappearing in the surrounding of the stopping locus. From the time interval of incoming and decaying particle the spectrum of the decay times is registered.

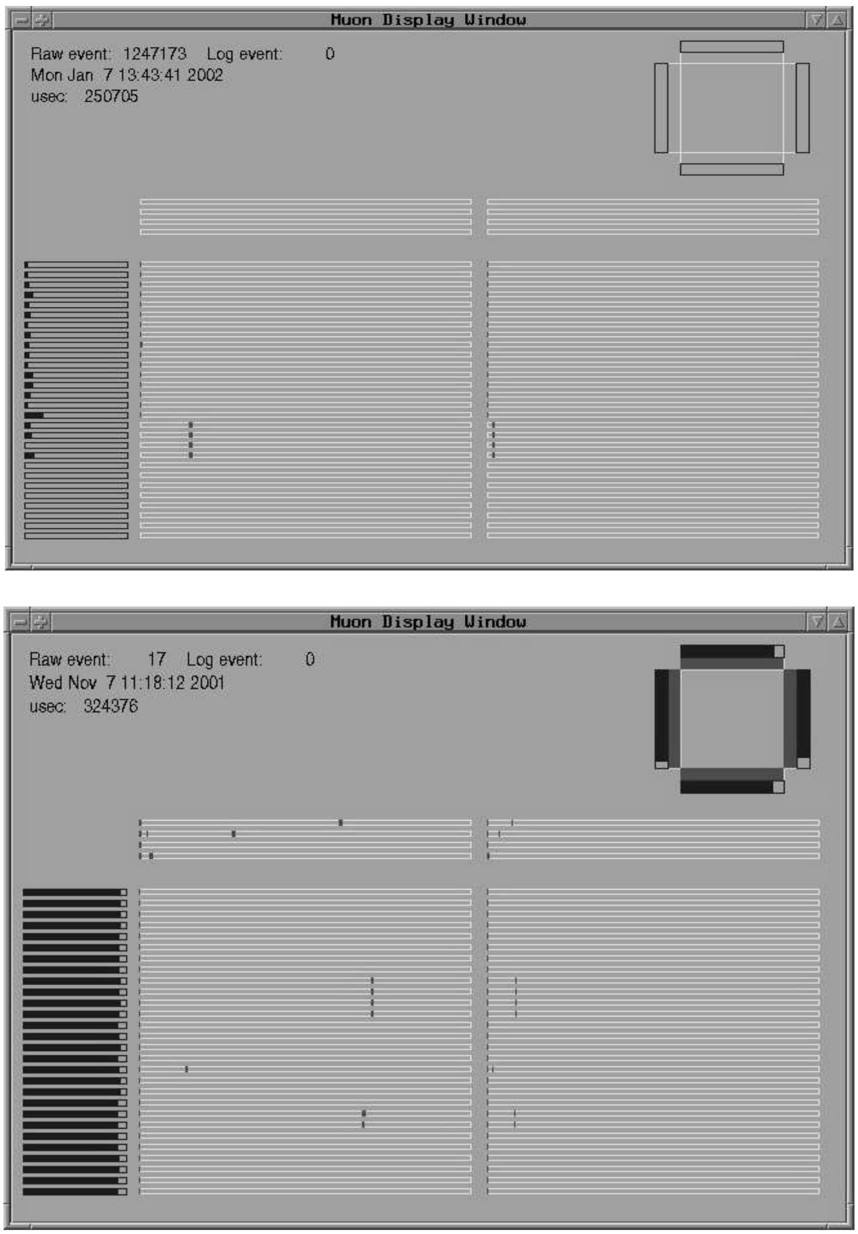

Fig.4 Graphical display of a "real" event

Fig. 4 shows two events; the left scale gives the anodic spectrum in arbitrary units; the right side presents the time signals using 2 time scales with 256 and 2048 channels, respectively. A good event is presented in **Fig. 4** (upper panel); the muon is stopped in the 8-th layer, the decay particle being emitted in the backward direction.
The good events are grouped in 8 classes, depending on the direction and the observed length of the electron track /3,4 /, see fig.5.

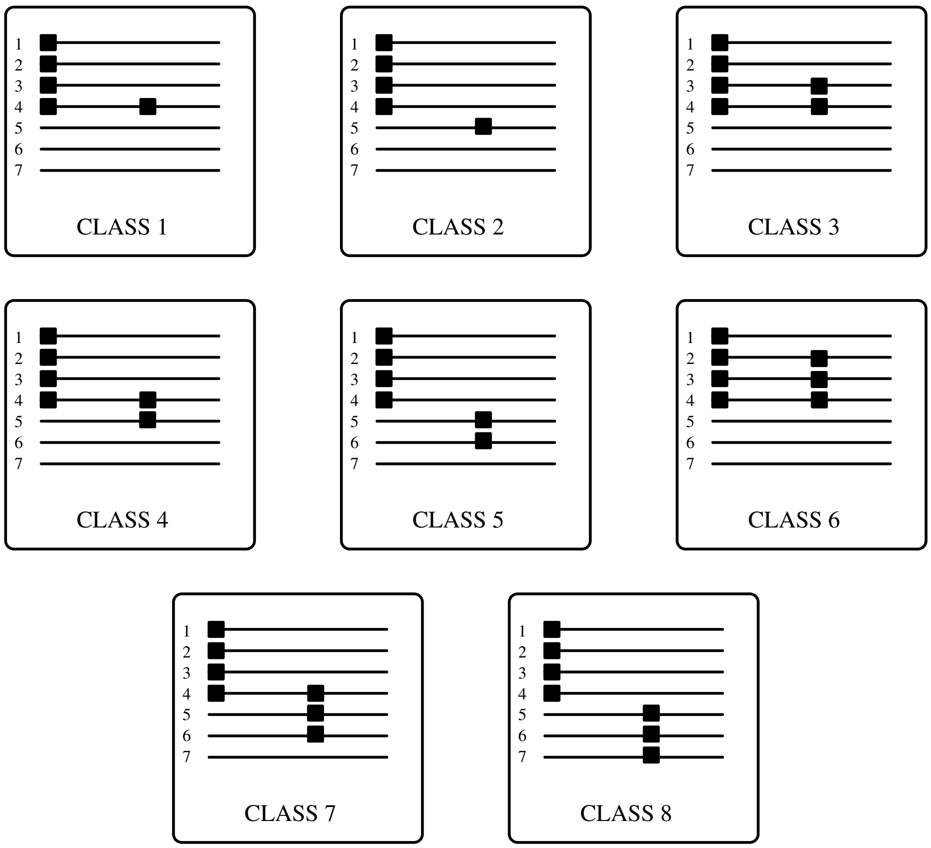

Fig.5 The classification of the events

The four VETO channels are shown above the active layers; a false event, entering from lateral side of the detector in one of the anti-coincidence layers, is immediately visualised and rejected, see fig.4 (bottom).

5. Charge ratio of muons of inclined incidence

As can be seen from the **Fig. 4**, the conditions for the events selection are the following:

- the two time signals from one scintillator plate have to be coincident in time,
- only events with two clearly subsequent particles are accepted,
- the muon track, with "zero" signal of each MTDC channel has to be continous from the first active modules down to the "stopping" layer,
- there is only one coincident particle which starts with some delay around the layer where the muon stopped,
- there is no signal in any of the 4 anti-counters on the side.

The selected number of good events which fulfill the cut conditions is about 1.5 millions events on each direction, leading to a considerable reduction of the events, but resulting in a maximum ratio of signal to noise, which is essential in the analysis. The exponential character of the measured decay curve is not influenced by such cuts, as the positive and negative muons are lost with equal probability.

The investigation of the zenith and azimuth dependence of the muon charge ratio have been started with measurements in the East and West direction (KAMIOKANDE convention: East means muons travelling to West) at a mean zenithal angle of 35^0, about 5 millions of events in each direction /9/.

Fig. 6 shows the acceptance of events for the energy, the zenith and azimuth incident angles of incidence.

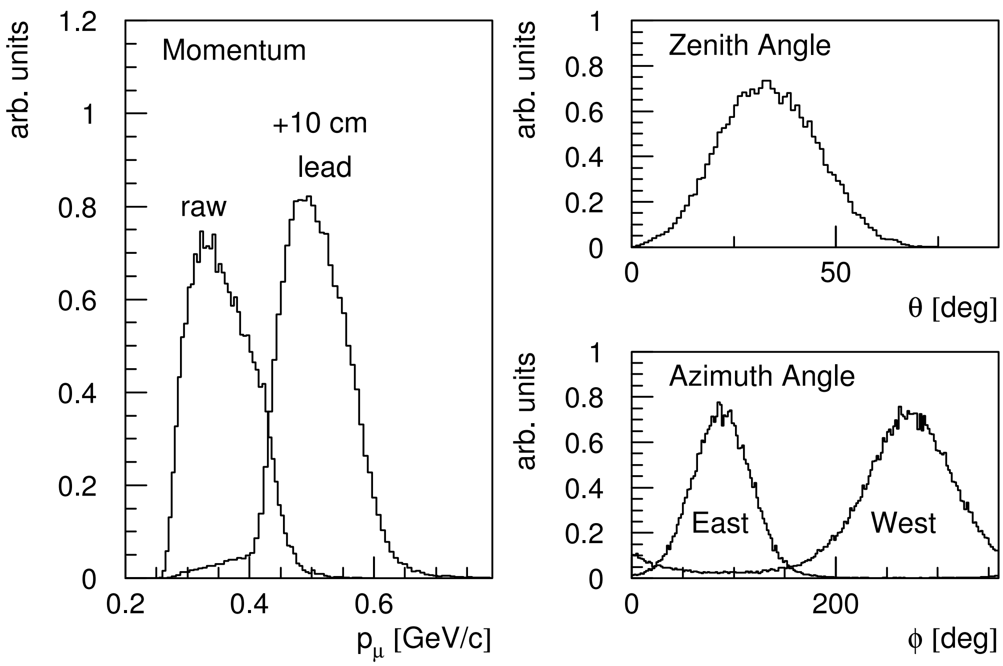

Fig.6 Acceptance in muon momentum and angle of incidence

A correct simulation of the detector response is crucial for getting a correct estimation of the value for the muon charge ratio. By simulations:

- the events are built in a similar way like the experimental ones and grouped in 8 classes of events depending on the layer in which the muon is stopped, the direction and the place where the emitted particle is stopped,
- the threshold conditions for the energy deposit in the active layers are fixed, and the detection efficiency coefficients are determined.

A check of the simulations is done by comparing the distributions of stopped muons over different layers and the relative frequencies of different classes from simulations with the experiment, see **Fig. 7**.

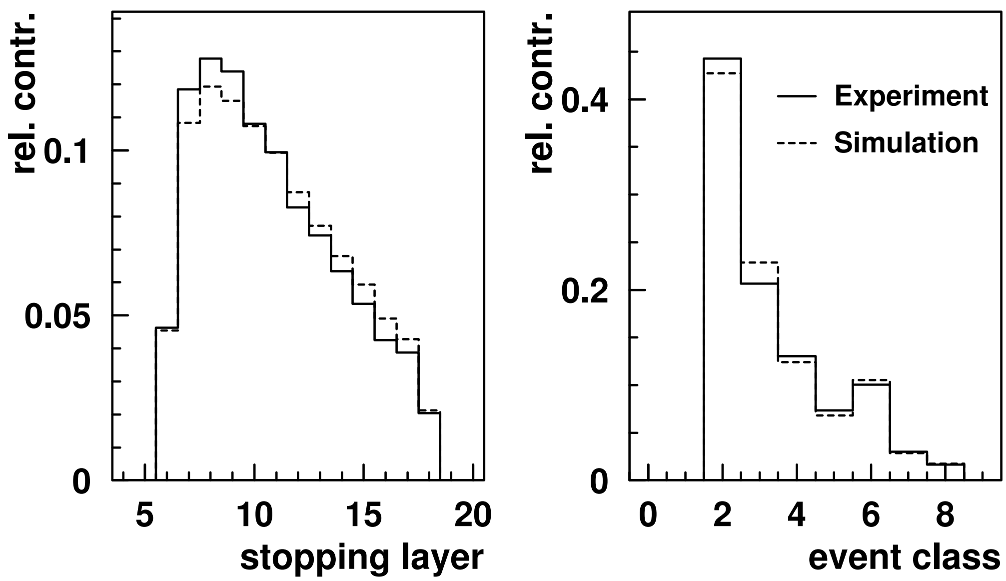

Fig.7 Comparison of experimental data (dashed line) to the simulations (solid-line) for the distributions of the muon stopped in the detector and the relative frequency of different event classes for the East direction of the Earth's magnetic field

Fig. 8 shows the results of the simulations indicating the exponential decay for different materials and the comparison of the experimental decay curve with the free decay of positive muons.

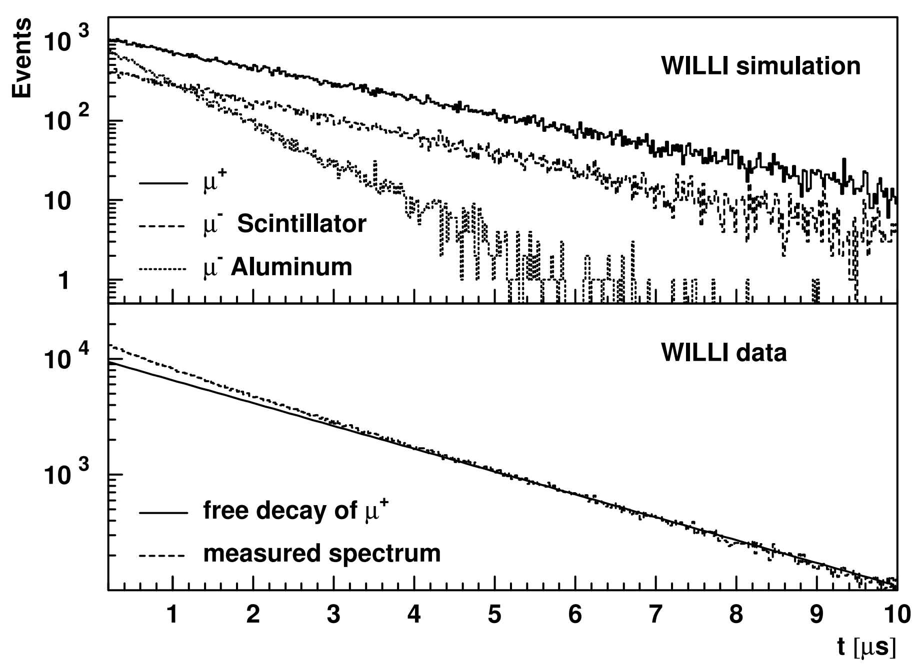

Fig.8 The muons decay curves, simulations and data

The simulation for muon fluxes have been performed with the CORSIKA code /10/ with special improvement for describing the low energy muons where the influence of the magnetic field becomes important /3/. Thus, the geomagnetic cut-off is taken into account by a detailed microscopic calculation /11/, the solar modulation is handled by the parametrization of Gleeson and Axford /12/ and the local magnetic field is tabulated on the basis of International Geomagnetic Reference Field /13/.

The **Fig. 9** (left) shows the comparison of the measured data of muon charge ratio for vertical and inclined muons with CORSIKA simulations, on basis of DPMJET II.5 model for describing hadronic interactions.

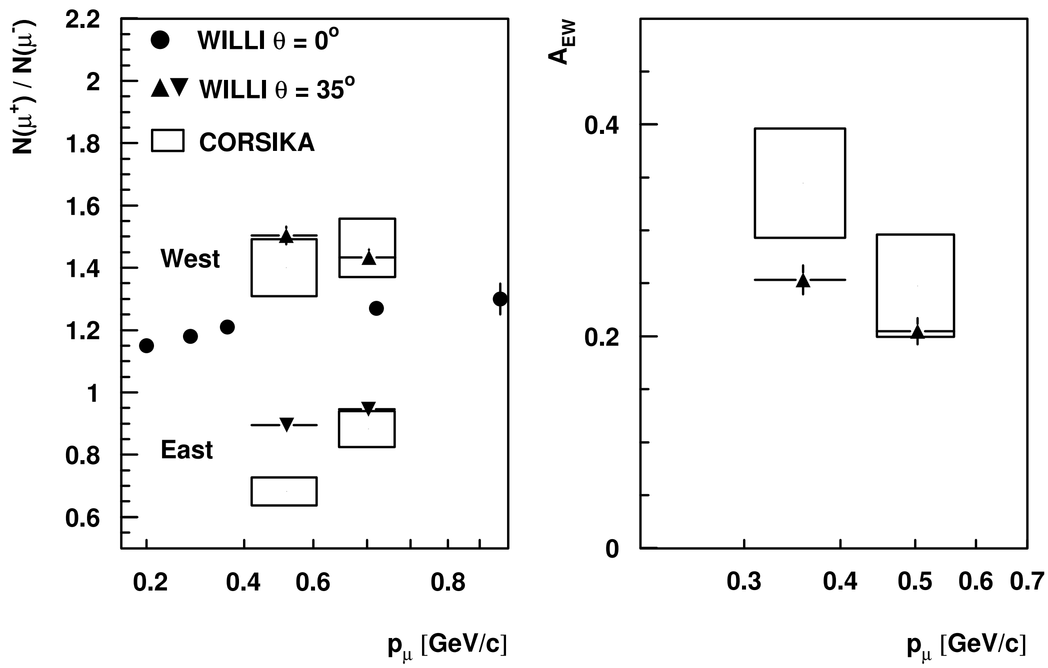

Fig.9 Energy dependence of the muon charge ratio and of the azimuthal anisotropy comparing experimental data and simulations

The measured muon charge ratio values for vertical muons show a smooth decrease with decreasing muon energy, the values of the charge ratio measured for inclined muons in the East and West direction being well placed under and above the corresponding values of their sum.

6. Azimuthal anisotropy

The East–West effect is expressed by the azimuthal anisotropy $A_\mu = (R_W - R_E)/(R_W - R_E)$, with R_W and R_E being the values of the muon charge ratio measured in the West and East direction and quantifies the effect .

Fig.9 (right) shows the azimuthal anisotropy the muon charge ratio, obtained in the measurements and in the simulations. Measurements of the asymmetry of the muon charge ratio in the East-West directions, observed with a mean zenith angle of 35^0, results in values of the asymmetry of the charge ratio decreasing from 0.25 to 0.20 in the muon momentum range of 0.35-0.50 GeV/c, relevant to the atmospheric neutrino anomaly.

In contrast to the anisotropy of neutrinos observed by KAMIOKANDE arising from the anisotropy of the primary cosmic flux /3/, the anisotropy of the muon flux in Bucharest could be attributed to the local magnetic field.

7. Concluding remarks

i. Our method to determine the muon charge ratio by measuring the lifetime of muons stopped in the matter /4,5/, overcomes the uncertainities appearing in measurements based on magnetic spectrometers, which are affected by systematic effects at low muon energies, due to problem in the particle and trajectory identification .

ii. The rotatable detector WILLI /9/ allows measurements of the charge ratio of muons with different angles of incidence enabling the determination of the East-West effect of the Earth's magnetic field, which deflects the trajectories of the charged particles in the atmosphere.

iii. Our measurements with rotatable WILLI, inclined at 45^0 show a pronounced East-West effect, in good agreement with simulation data /3/ and with the East-West effect found in neutrino measurements /14/.

iv. The measurements of East-West effect in muon charge ratio permit to verify the hadronic interaction models in simulating neutrino and muon fluxes, the geometry of detection in a complex sphere and the influence of geomagnetic cut- off and the local magnetic field.

References

1. J.Wentz et al. : J.Phys.G.Nucl.Part.Phys, 27 (2001) 1699
2. Y.Fukuda et al.: Phys.Lett.B433 (1998)9; Phys.Rev.Lett 81 (1988) 1562
3. J.Wentz et al.: Phys.Rev.D67 (2003) 073020
4. B.Vulpescu al.: Nucl.Instr.& Meth. in Phys.Res. A414 (1998) 205
5. B. Vulpescu et al.: J.Phys.G.Nucl.Part.Phys, 27 (2001) 977
6. I.M.Brancus et al. : Report WP17 IDRANAP 18-02 (2002)
7. CERN 1994 GEANT3.21 Program Library Long Writeup W5013
8. J.Kramer et al.: Phys.Rev.Lett.83 (1999) 4241
9. I.M.Brancus et al.: Proc.PANIC (2002)
10. D.Heck et al.: Report FZKA 6019 (1998)
11. J.Wentz et al.: Proc.27-th ICRC (2001) p.4213
12. L.Gleeson, W.Axford: Astrophys.Journ.154 (1968) 1011
13. National Geographic Data Center, Data Announcement 88-MGG-02 (1988)
14. T.Futagami et al.: Phys.Rev.Lett.82 (1999) 5194